



# Influence of operating parameters on surface properties of RF glow discharge oxygen plasma treated TiO<sub>2</sub>/PET film for biomedical application



K. Navaneetha Pandiyaraj<sup>a,\*</sup>, R.R. Deshmukh<sup>b</sup>, R. Mahendiran<sup>a</sup>, Pi-G Su<sup>c</sup>, Emre Yassitepe<sup>d</sup>, Ismat Shah<sup>d</sup>, Stefano Perni<sup>e</sup>, Polina Prokopovich<sup>e,f</sup>, Mallikarjuna N. Nadagouda<sup>g</sup>

<sup>a</sup> Surface Engineering Laboratory, Department of Physics, Sri Shakthi Institute of Engineering and Technology, L&T by pass, Chinniyam Palayam (post), Coimbatore 641062, India

<sup>b</sup> Department of Physics, Institute of Chemical Technology, Matunga, Mumbai 400 019, India

<sup>c</sup> Department of Chemistry, Chinese Culture University, Taipei 111, Taiwan

<sup>d</sup> Department of Physics and Astronomy, Department of Materials Science and Engineering, University of Delaware, 208 Dupont Hall, Newark, United States

<sup>e</sup> School of Pharmacy and Pharmaceutical Sciences, Cardiff University, Cardiff, UK

<sup>f</sup> Institute of Medical Engineering & Medical Physics, School of Engineering, Cardiff University, UK

<sup>g</sup> The U.S. Environmental Protection Agency, ORD, NRMRL, WSWRD, 26W. Martin Luther King Drive, Cincinnati, OH 45268, USA

## ARTICLE INFO

### Article history:

Received 21 June 2013

Received in revised form 31 October 2013

Accepted 12 December 2013

Available online 18 December 2013

### Keywords:

RF glow discharge oxygen plasma

TiO<sub>2</sub>/PET

Surface properties

Antibacterial adhesion

Cell compatibility

## ABSTRACT

In this paper, a thin transparent titania (TiO<sub>2</sub>) film was coated on the surface of flexible poly(ethylene terephthalate) (PET) film using the sol–gel method. The surface properties of the obtained TiO<sub>2</sub>/PET film were further improved by RF glow discharge oxygen plasma as a function of exposure time and discharge power. The changes in hydrophilicity of TiO<sub>2</sub>/PET films were analyzed by contact angle measurements and surface energy. The influence of plasma on the surface of the TiO<sub>2</sub>/PET films was analyzed by atomic force microscopy (AFM) as well as the change in chemical state and composition that were investigated by X-ray photo electron spectroscopy (XPS). The cytotoxicity of the TiO<sub>2</sub>/PET films was analyzed using human osteoblast cells and the bacterial eradication behaviors of TiO<sub>2</sub>/PET films were also evaluated against *Staphylococcus* bacteria. It was found that the surface roughness and incorporation of oxygen containing polar functional groups of the plasma treated TiO<sub>2</sub>/PET films increased substantially as compared to the untreated one. Moreover the increased concentration of Ti<sup>3+</sup> on the surface of plasma treated TiO<sub>2</sub>/PET films was due to the transformation of chemical states (Ti<sup>4+</sup> → Ti<sup>3+</sup>). These morphological and chemical changes are responsible for enhanced hydrophilicity of the TiO<sub>2</sub>/PET films. Furthermore, the plasma treated TiO<sub>2</sub>/PET film exhibited no cytotoxicity against osteoblast cells and antibacterial activity against *Staphylococcus* bacteria which can find application in manufacturing of biomedical devices.

© 2013 Elsevier B.V. All rights reserved.

## 1. Introduction

Currently, polymeric materials are employed in the biomedical industry for artificial organs, medical devices and disposable clinical apparatus due to their versatility in producing devices with remarkably different mechanical and physical properties. However, the major complications of polymeric materials are the infection of bacteria, when the materials are implanted in the human body. The bacterial adhesion causes a high rate of morbidity and mortality thereby significantly increasing health care costs [1–4]. Hence polymeric materials need some additional treatment to improve their antibacterial and biological properties. As the surface properties of the materials play a vital role in determining their bioactivity and long term performance *in vivo* [5,6], surface

modification techniques are found to be useful in this field. Several surface modification techniques such as corona discharge, glow discharge plasma treatment, chemical etching, incorporation of silver nano particles, surface-immobilized polyethylene oxide (PEO), surface thiocyanation, mechanical and thermal treatments have been employed to improve the surface and biological properties of the polymeric materials [7–13]. Among them, glow discharge plasma treatment has been found to be an extremely attractive way to modify the surface properties of polymeric materials through surface functionalization, cross linking, degradation or a combination of these processes. Furthermore, the glow discharge plasma processes are precisely controllable, conformal and the surface chemistry can be tailored for the required end use. An interesting feature of glow discharge plasma treatment is that the changes are confined to a depth of a few nanometers at the surface because of the low level of penetration and also there is a dry reaction in the gas–solid phase. Depending on the gas composition and treatment conditions, ions, electrons, fast neutrals, radicals and UV radiation

\* Corresponding author. Tel.: +91 9003590874 (mobile).  
E-mail addresses: [dr.knpr@gmail.com](mailto:dr.knpr@gmail.com) (K.N. Pandiyaraj),  
[Nadagouda.Mallikarjuna@epamail.epa.gov](mailto:Nadagouda.Mallikarjuna@epamail.epa.gov) (M.N. Nadagouda).

contribute to the polymer treatment, resulting in the enhancement of the surface properties of materials [10–16]. This kind of treatment saves water and energy and does not pollute the environment.

Titanium dioxide (TiO<sub>2</sub>) is widely used in biomedical implants such as hip and knee prostheses, heart valves etc. TiO<sub>2</sub> is also used as coatings on eye-glasses, flat panel displays and different optical systems due to its superior mechanical properties, chemical stability, biocompatibility and lack of toxicity. The synthesis method to produce TiO<sub>2</sub> thin films and the substrate on which it is deposited is known to play an important role for design efficacy of a biomaterial [17,18]. For example TiO<sub>2</sub> films coated on hard surfaces such as glass and stainless steel are generally not suitable for the production of artificial implants [14–19]. Soft matter substrates such as polypropylene (PP), polyethylene (PE), poly (ethylene terephthalate) (PET) and polycarbonate (PC) are increasingly being considered for tissue and organ replacements [20–23]. PET in particular is one of the most significant polymeric materials being used for the production of biomedical materials because of its excellent mechanical properties and moderate biocompatibility. Especially, it is widely adopted in cardiovascular implants, such as artificial heart valves and blood vessels.

In this work, transparent TiO<sub>2</sub> films were coated on the surface of PET polymers by simple sol–gel technique. The surface properties of the obtained TiO<sub>2</sub>/PET films were further improved by radio frequency (RF) glow discharge oxygen plasma as a function of discharge power and exposure time. The films were characterized using contact angle measurements, atomic force microscopy and X-ray photo electron spectroscopy for hydrophilicity, surface morphology and chemical analysis respectively. The influence of surface modification on antibacterial properties was assessed by bacterial eradication tests with *Staphylococcus* bacteria and its cytotoxicity determined on human osteoblast cells.

## 2. Materials and methods

### 2.1. Materials

Titanium isopropoxide (Ti (O-i-C<sub>3</sub>H<sub>7</sub>)<sub>4</sub>) was purchased from Alfa Aesar, India and biaxial oriented PET films of 100- $\mu$ m thickness were kindly supplied by Garware Polyester PVT Ltd., India. Other chemicals such as nitric acid, acetone and ethanol were obtained from MERCK, India. The PET film was cut into 5 cm  $\times$  5 cm pieces and washed ultrasonically in acetone followed by distilled water for 1 h and then dried at room temperature before using them for TiO<sub>2</sub> coating and plasma treatment.

### 2.2. Immobilization of titania (TiO<sub>2</sub>) on PET surface

Transparent TiO<sub>2</sub> films were immobilized on the surface of PET films through titanium isopropoxide sol by a simple dip coating technique. Initially, 1 mol titanium isopropoxide dissolved in 9 mol of ethanol was vigorously stirred for 2 h at 0 °C and then a mixture of water (1 mol) and HNO<sub>3</sub> (0.1 mol) was added drop wise to the above solution with a burette under stirring. The resultant alkoxide solution was kept standing at 45 °C temperature for hydrolysis reaction for 36 h, resulting in the TiO<sub>2</sub> sol. PET films were used as the substrate for the thin film deposition. Before TiO<sub>2</sub> immobilization, PET substrates were cleaned ultrasonically in distilled water and acetone for 45 min and dried at room temperature. After that the PET film was subjected to oxygen plasma for 15 min, the working pressure and discharge power were 0.2 mbar and 30 W respectively for improvement of hydrophilicity of PET films which in turn enhances the adsorption strength of the TiO<sub>2</sub> on the surface of the PET films. Finally the oxygen plasma treated PET films were dipped in the TiO<sub>2</sub> precursor solution following dipping withdrawing cycles at 25 °C and then dried in air at the temperature of 85 °C for 24 h resulting in the TiO<sub>2</sub> being immobilized on the surface of the PET films. Subsequently TiO<sub>2</sub>/PET films were washed with distilled water for 20 min to remove the excess TiO<sub>2</sub> particles from the PET surfaces. The thickness of the TiO<sub>2</sub> layer on the PET film was measured using

**Table 1**  
Surface tension components of the testing liquids.

Liquids	$\gamma_l$ (mJ/m <sup>2</sup> )	$\gamma_l^p$ (mJ/m <sup>2</sup> )	$\gamma_l^d$ (mJ/m <sup>2</sup> )
Water (W)	72.8	51.0	21.8
Formamide (F)	58.2	18.7	39.5
Ethylene glycol (EG)	48.0	19.0	29.0

Mitutoyo SurfTest SJ-301 profilometer and was found to be 350 nm. During the thickness measurement, we have not observed any irregularity and porous structure on the surface of TiO<sub>2</sub>/PET films which clearly revealed the compactness and uniformity of the same. The obtained TiO<sub>2</sub>/PET films were further treated by RF glow discharge oxygen plasma. The plasma reactor consists of a plasma chamber made of glass with length of 45 cm and diameter of 7.5 cm. The system has two aluminum electrodes having the dimension of 22 cm  $\times$  3.5 cm  $\times$  0.1 cm placed externally at 8.5 cm apart and were capacitively coupled to a radio frequency power supply ( $\nu = 13.56$  MHz). The sample was kept on the glass sample holder placed inside the chamber. Before the plasma treatment, the chamber was initially evacuated to a pressure of  $\sim 10^{-3}$  mbar using a rotary pump (EDWARDS) and the same was measured by Pirani gauge. Precursor gas (oxygen) was purged 3 times and the working pressure was adjusted to 0.15 mbar using a needle valve. The RF power was applied between the two electrodes to generate stable glow discharge. Finally the samples were treated at different exposure times, discharge power at a fixed pressure level of 0.15 mbar and electrode separation of 8.5 cm.

### 2.3. Surface analysis

The surface hydrophilicity of the plasma treated TiO<sub>2</sub>/PET films was analyzed using sessile drop contact angle measurements [16,20,21], with three different liquids such as distilled water (W), formamide (F) and ethylene glycol (EG) of known surface tension components (Table 1) [15,16]. The error in the measurement was found to be  $\pm 2^\circ$ . The contact angle measurements were made under controlled room temperature and humidity conditions.

Further, the polar ( $\gamma_s^p$ ) and disperse ( $\gamma_s^d$ ) components of the TiO<sub>2</sub>/PET films were estimated using Fowkes approximation extended by Owens-Wendt as follows [16,20,21,24].

$$\left[ \frac{1 + \cos\theta}{2} \right] \times \left[ \frac{\gamma_l}{\sqrt{\gamma_l^d}} \right] = \sqrt{\gamma_s^p} \times \sqrt{\frac{\gamma_l^p}{\gamma_l^d}} + \sqrt{\gamma_s^d} \quad (1)$$

Eq. (1) is in the form:

$$Y(\text{LHS}) = m \cdot X(\text{RHS}) + C \quad (2)$$

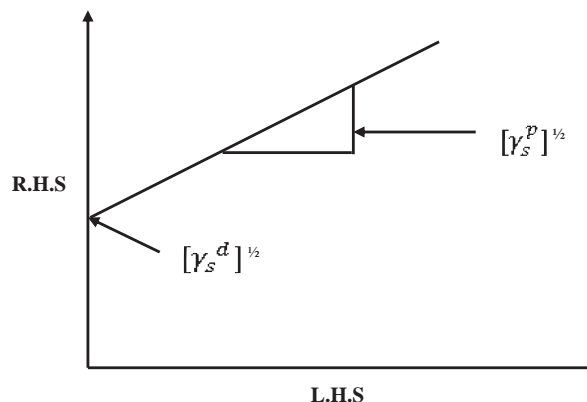
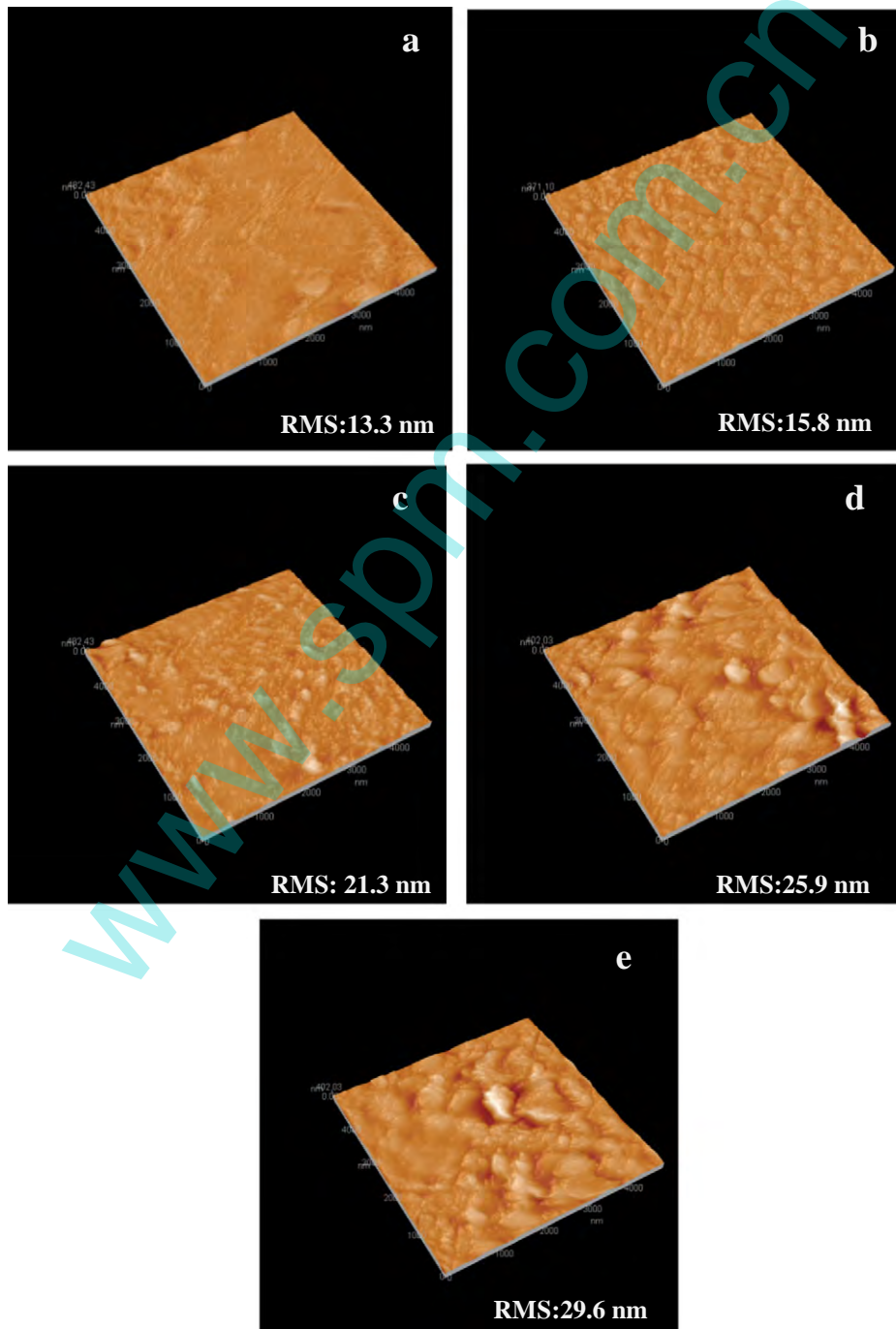


Fig. 1. Plot of Fowkes equation to estimate solid surface free energy.

**Table 2**Variation of contact angle and surface energy with time for plasma treated TiO<sub>2</sub>/PET films at different power levels.

Power (W)	Exposure time (min)	Contact angle (degree)			Surface energy components (mJ/m <sup>2</sup> )		
		W	F	EG	$\gamma_s^p$	$\gamma_s^d$	$\gamma_s$
30	0	65.2	58.3	48.2	23.67	12.61	36.29
	2	58.6	50.1	45.4	28.09	12.88	40.97
	5	51.3	41.4	36.7	32.49	14.15	46.64
	10	35.8	29.6	22.9	46.24	11.74	57.98
	15	28.1	20.2	18.2	51.98	11.36	63.35
45	0	65.2	58.3	48.2	23.67	12.61	36.29
	2	50.4	41.7	35.4	33.87	13.58	47.45
	5	42.6	36.4	30.6	41.99	11.65	53.64
	10	29.1	23.7	18.1	52.18	10.89	63.07
	15	22.7	17.3	14.7	56.25	10.24	66.49

**Fig. 2.** AFM images of the O<sub>2</sub> plasma treated TiO<sub>2</sub>/PET films (a) untreated, (b) 2, (c) 5, (d) 10, and (e) 15 min at the power level of 30 W.

where the value of LHS and RHS could be obtained by contact angle value ( $\theta$ ), surface tension of testing liquids ( $\gamma_l$ ), polar ( $\gamma_l^p$ ) and disperse ( $\gamma_l^d$ ) components of liquid surface tension used from Table 1. The plot of LHS vs RHS gave a straight line with intercept on Y-axis (Fig. 1). The slope and intercept obtained from the plot were squared and added up to give a total solid surface free energy ( $\gamma_s$ ) of the TiO<sub>2</sub>/PET films as given in Eq. (3).

$$\gamma_s = \gamma_s^p + \gamma_s^d \quad (\text{mJ/m}^2) \quad (3)$$

The surface morphology of the TiO<sub>2</sub>/PET films was evaluated using Seiko Instruments Scanning force microscopy (AFM, Ben-Yuan, CSPM

4000) operated in tapping mode with horizontal and vertical resolution of 0.26 and 0.10 nm respectively. Change in surface roughness of the plasma treated TiO<sub>2</sub>/PET films was expressed as a difference in the root mean square (RMS) of the vertical Z-dimension values within the examined areas, which was calculated using the following equation [25].

$$\text{RMS}_{xy} = \sqrt{\sum_{x,y=1}^N \frac{(Z_{x,y} - Z_{\text{average}})^2}{N}} \quad (4)$$

where  $Z_{\text{average}}$  is the average Z value within the examined area,  $Z_{x,y}$  is the local Z value and N indicates the number of points within the area.

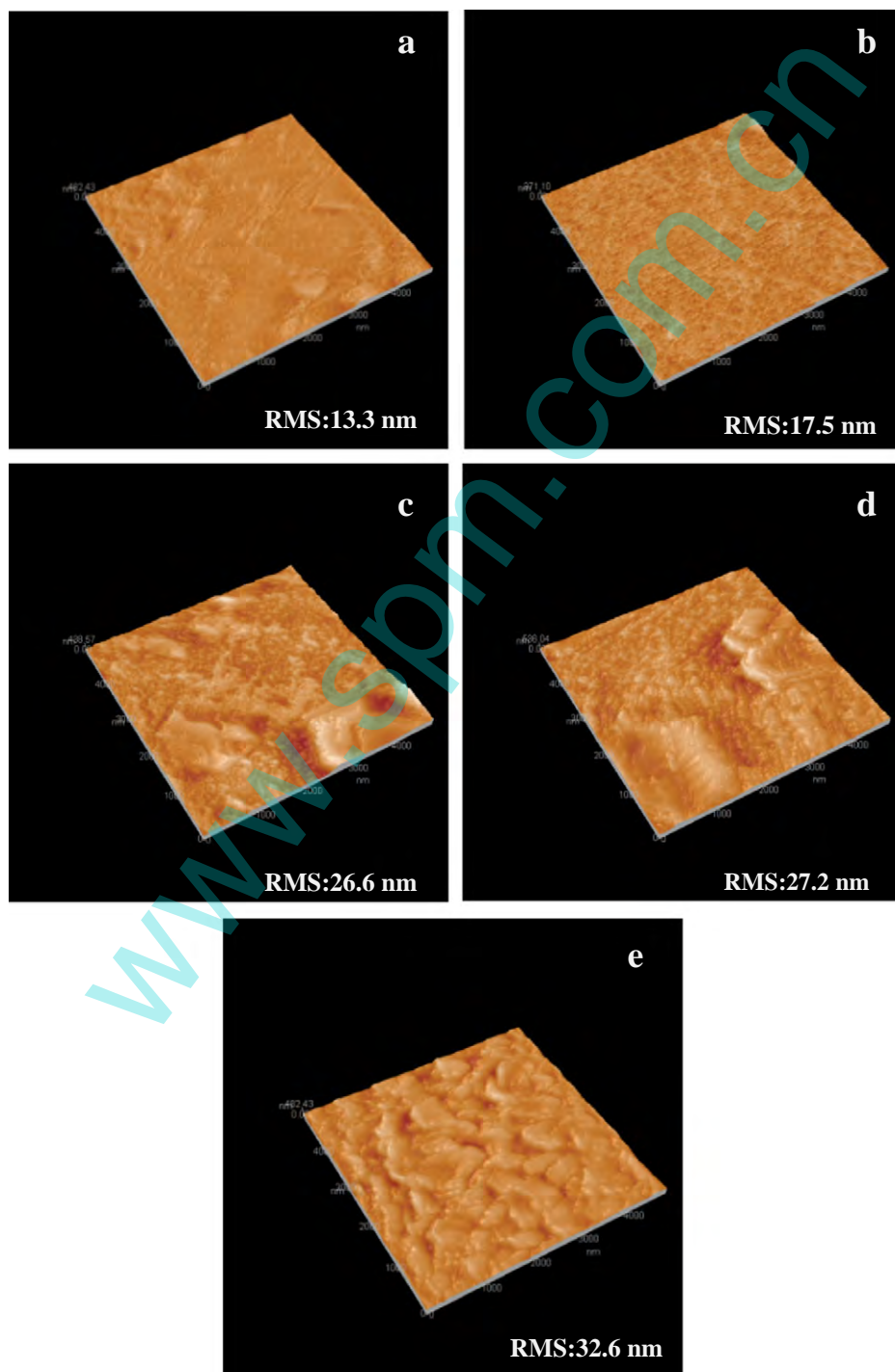


Fig. 3. AFM images of the O<sub>2</sub> plasma treated TiO<sub>2</sub>/PET films (a) untreated, (b) 2 min (c) 5 min, (d) 10 min and (e) 15 min at the power level of 45 W.



The change in chemical state of the TiO<sub>2</sub>/PET films induced by the oxygen plasma treatment was examined using X-ray photo electron spectroscopy (Omicron Surface Science Instruments with EAC2000-125 Energy Analyzer). Monochromatic AlK $\alpha$  X-rays (1486.7 eV) was employed. Typical operating conditions for the X-ray source were a 400- $\mu$ m nominal X-ray spot size (full width at half-maximum) at 15 kV, 8.9 mA, and 124 W for both survey and high resolution spectra. The C1s, Ti2p, and O1s envelopes were analyzed and peak-fitted using a combination of Gaussian and Lorentzian peak shapes obtained from XPSPEAK41 software package.

#### 2.4. Bacterial adhesion analysis

The antibacterial activity of the TiO<sub>2</sub>/PET films was analyzed using *Staphylococcus* bacteria. Prior to analysis, the PET, TiO<sub>2</sub>/PET and plasma processed TiO<sub>2</sub>/PET samples were washed with acetone and ethanol and then the samples were dried at room temperature. After this they were immersed in a bacterial suspension which was incubated at 37 °C temperature for 24 h. After incubation, the samples were washed with 20 ml of 0.87% NaCl solution containing polysorbate 80 at a pH of 7. Afterwards the growth of the bacteria on the TiO<sub>2</sub>/PET surface was analyzed using Optical microscopy.

#### 2.5. Cytotoxicity analysis

The cytotoxicity of untreated and plasma treated TiO<sub>2</sub>/PET films was analyzed using osteoblast cells. The osteoblast cells were cultured in Dulbecco's Modified Eagle's medium supplemented with fetal bovine serum (10% v/v) in an incubator at 37 °C in humidified atmosphere with 5% CO<sub>2</sub>. Cells were grown till confluence, washed twice with sterile PBS and detached with trypsin; osteoblast cells were counted (using trypan blue to differentiate between viable and no-viable cells) and a solution containing 10<sup>5</sup> cells/ml was prepared diluting with PBS. TiO<sub>2</sub>/PET film samples (1 × 1 cm) were placed in 24-well plates and 1 ml of solution containing osteoblast, prepared as described above, was added. The samples were incubated at 37 °C in humidified atmosphere with 5% CO<sub>2</sub> for two days. After that the samples were removed from the cultured medium and washed with PBS twice. The obtained samples were further placed in clean 24-well plate with 1 ml fresh medium. The MTT assay kit (Invitrogen, UK) was used to measure the cell viability of the samples. The MTT solution was prepared as per manufacturer guidance and added to the samples. The samples were incubated for 2 h and then the MTT solubilization solution was added; after dissolution of the crystals, the absorbance of each sample was recorded at 540 nm. The results are presented as the averages and standard deviations of three independent samples.

The cell viability is linked to the activity of the enzyme responsible for the reduction of MTT to purple formazan, the latter concentration is measured spectrophotometrically. The higher the reading, the higher the formazan produced, therefore, the higher the amount of enzyme presented and, consequently, the higher the number of cells.

### 3. Results and discussion

#### 3.1. Hydrophilic analysis: contact angle and surface energy results

The extent of hydrophilic modification of TiO<sub>2</sub>/PET films was measured by contact angle analysis using three different test liquids such as water, formamide, ethylene glycol. The variations in contact angle with the plasma treatment time at 30 and 45 W are shown in Table 2. It was observed that the contact angle value of the PET substrate was 89.6° for distilled water, 80.5° for formamide and 75.2° for ethylene glycol and it decreased considerably after TiO<sub>2</sub> coating (UT sample). The contact angle of TiO<sub>2</sub>/PET films with respect to all the three liquids decreased considerably at an exposure time of 5 min; it further decreased with increasing exposure time, for a given power level reaching the

lowest contact angle value of 22.7°, 17.3° and 14.7° for W, F and EG respectively after 15 min of plasma treatment. The lowest contact angle value was observed for the TiO<sub>2</sub>/PET film treated under a higher power level of 45 W compared with 30 W of discharge power (Table 2). The decrease in the contact angle is an indication of the formation of high magnitude of oxygen containing polar groups onto the surface of TiO<sub>2</sub>/PET film due to plasma treatment and also an increase in surface roughness of the same. The PET film used in the present investigation is of 100  $\mu$ m. The surface modification achieved during plasma treatment is just ~10 nm as reported in the literature [23,26]. It means that in our case one part in ten thousand is modified. Also the power used in the present experiment is very low (30 and 45 W). The electrodes are kept outside the tubular plasma reactor with 8.5 cm distance between them, which is quite a large distance. Therefore, for bulk property—the mechanical strength remains unchanged. In the past, we have tested gaseous plasma treated samples randomly for their mechanical properties and have found no adverse effect. Therefore, in the present experiment we have not measured this parameter. The factors, surface roughness and functional changes facilitate the surface of TiO<sub>2</sub>/PET film to become highly hydrophilic in nature related to the untreated one [16,21,26–29].

Changes in polar and dispersive components of the total surface energy of untreated and plasma treated TiO<sub>2</sub>/PET films were estimated using Fowkes approximation from contact angle measurements data. The surface energy of the PET film was found to be 26.84 mJ/m<sup>2</sup>, whereas its polar and disperse components were 5.89 mJ/m<sup>2</sup> and 20.95 mJ/m<sup>2</sup> respectively and they increased considerably after TiO<sub>2</sub> coating (untreated sample). The surface energy of the unmodified TiO<sub>2</sub>/PET film was found to be 36.29 mJ/m<sup>2</sup>. The surface energy value increased with increase in plasma treatment time at a given power and reached the maximum value of 66.49 mJ/m<sup>2</sup> for the sample (TiO<sub>2</sub>/PET) treated at the higher power level of 45 W (Table 2). The increase in total surface energy was essentially due to the incorporation of polar components ( $\gamma_s^p$ ), whereas, there was no appreciable change in the dispersive component ( $\gamma_s^d$ ) of the surface. The above changes may be due to the increase in power level leading to an increase in the degree of ionization of plasma that resulted in an enhancement of the active species concentration. The strong interaction between active species and TiO<sub>2</sub>/PET produces active sites on the material surface leading to an increase in the formation of the oxygen containing polar groups onto the TiO<sub>2</sub>/PET surfaces. The properties such as wettability, biocompatibility, cell compatibility and antibacterial strongly depend upon the surface energy of TiO<sub>2</sub>/PET films.

#### 3.2. Surface topographical analysis: AFM results

The surface topography of the materials could play a vital role in improving the biocompatibility of an implant. Fig. 2a–e shows AFM images of TiO<sub>2</sub>/PET films as a function of exposure time at an operating power of 30 W. The surface of the TiO<sub>2</sub>/PET untreated film was relatively smoother and has moderate roughness which exhibits the uniform distribution of TiO<sub>2</sub> layer on the surface of the PET film as shown in Fig. 2a. Even a

**Table 3**

The surface elemental composition and ratio of the plasma modified TiO<sub>2</sub>/PET film for different exposure times.

Power (W)	Exposure time (min)	Elemental composition (at %)			Elemental ratio	
		C	O	Ti	C/Ti	O/C
30	0	45.1	50.1	4.8	9.39	1.11
	10	41.19	52.21	6.6	6.24	1.26
	15	34.92	54.7	10.38	3.36	1.56
45	0	45.1	50.1	4.8	9.39	1.43
	5	36.1	53.94	9.96	3.62	1.49
	10	31.7	55.25	13.05	2.42	1.74
	15	25.25	58.8	15.95	1.58	2.32

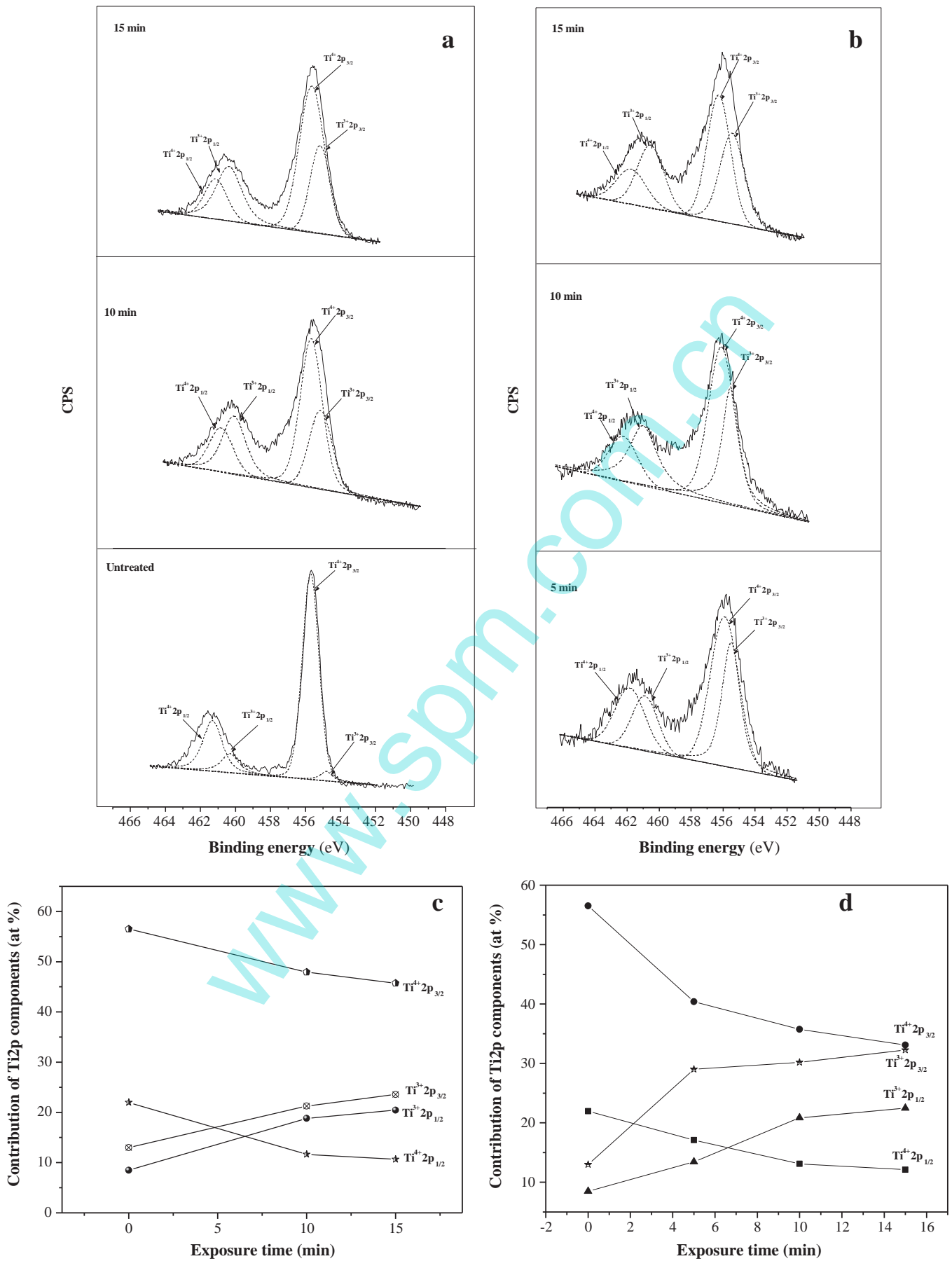


Fig. 4. XPS Ti2p spectra and contribution of Ti2p components of O<sub>2</sub> plasma treated TiO<sub>2</sub>/PET film surfaces for different power levels of 30 W (a & c) and 45 W (b & d).

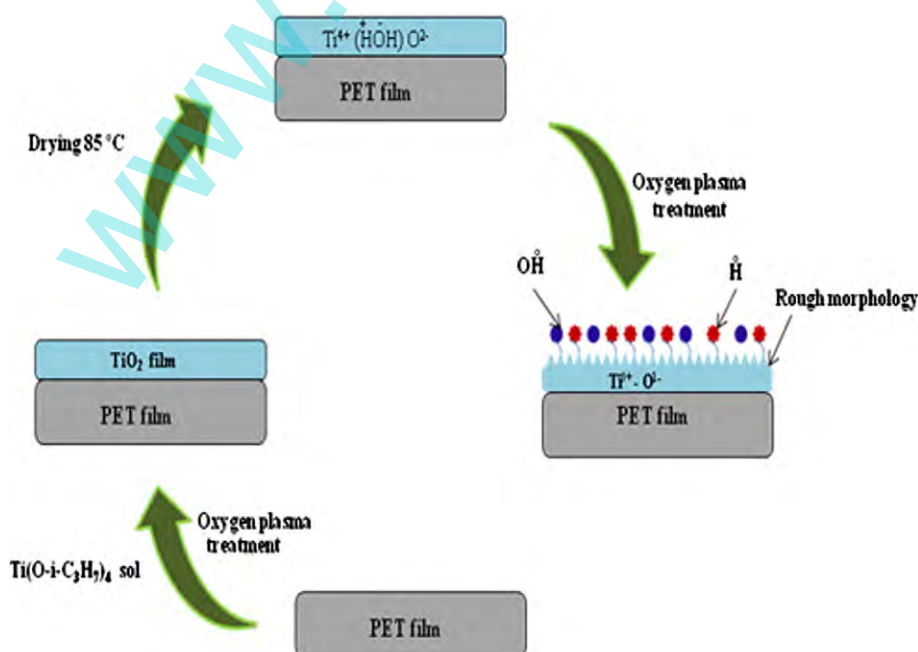
short duration (2 min) of plasma treatment results in rougher morphology. These topographical changes were further increased with increasing exposure times, as can be seen in Fig. 2b–e. A similar trend was observed when the samples were treated at higher power level of 45 W. However, the samples exhibited enhanced rougher morphology when treated at 45 W which may be due to the magnitude of bombardment of more energetic plasma species on the surface that leads to the increase in surface roughness of the TiO<sub>2</sub>/PET films at the higher discharge power level (Fig. 3b–e). Moreover, the RMS value of surface roughness of the untreated TiO<sub>2</sub>/PET film was 13.3 nm and gradually increased with increasing exposure time. However, the maximum value of the RMS surface roughness was obtained at the discharge power of 45 W for all the treatment times compared with the samples treated at the power level of 30 W. This phenomenon is related with the etching process by plasma particles. The results indicated an apparent increase in the surface roughness and effective surface area for contact, causing improvement in the hydrophilicity of the materials.

### 3.3. Surface composition analysis: XPS results

The elemental composition of the untreated and plasma treated TiO<sub>2</sub>/PET films is presented in Table 3 which mainly contain C1s, O1s and Ti2p. It is clear from Table 3 that the carbon content decreases whereas there is an increase in oxygen and Ti2p contents with increase in plasma treatment time. The higher concentration of O1s and Ti2p was obtained for the sample exposed at the higher power level of 45 W. The above change revealed the incorporation of significant amount of O1s onto the surface of the TiO<sub>2</sub>/PET films when treated by oxygen plasma. Table 3 also shows the ratio of the O1s/C1s and C/Ti of the untreated and plasma treated TiO<sub>2</sub>/PET films. It is clearly seen that the O/C ratio has increased with respect to the increase in exposure time which may be attributed to the increase in the newly formed oxygen functional groups by oxygen plasma treatment [30]. Furthermore, the ratio of C/Ti in the TiO<sub>2</sub>/PET film was decreased steadily with the increase in exposure time. The changes may be attributed to the removal of the carbon atom from the surface of the plasma treated TiO<sub>2</sub>/PET film surface. The introduction of oxygen containing functional groups onto the TiO<sub>2</sub>/PET surface may be the main reason for the improvement of the hydrophilic property and biological response.

Information on how the chemical states of TiO<sub>2</sub>/PET films were modified as a consequence of oxygen plasma treatment can be obtained from deconvolution of XPS signals using the Gaussian–Lorentzian fit. Fig. 4 shows the Ti2p core level of the untreated and plasma treated TiO<sub>2</sub>/PET film for different treatment times at 30 and 45 W. The peaks may be identified for the untreated TiO<sub>2</sub>/PET to be at 454.9 eV due to Ti<sup>3+</sup>2p<sub>3/2</sub>, at 455.8 eV due to Ti<sup>4+</sup>2p<sub>3/2</sub>, at 460.4 eV due to Ti<sup>3+</sup>2p<sub>1/2</sub> and at 462.4 eV due to Ti<sup>4+</sup>2p<sub>1/2</sub>. The Ti2p XPS spectrum of the plasma treated TiO<sub>2</sub>/PET was also fitted with four peaks at 455.0, 456.6, 460.2 and 462.2 eV due to Ti<sup>3+</sup>2p<sub>3/2</sub>, Ti<sup>4+</sup>2p<sub>3/2</sub>, Ti<sup>3+</sup>2p<sub>1/2</sub> and Ti<sup>4+</sup>2p<sub>1/2</sub> respectively [31–34]. However, the intensity of the peaks due to Ti<sup>3+</sup>2p<sub>3/2</sub> and Ti<sup>3+</sup>2p<sub>1/2</sub> was increased by an increase in the exposure time whereas there is a decrease in the chemical state of Ti<sup>4+</sup> (Ti<sup>4+</sup>2p<sub>3/2</sub> and Ti<sup>4+</sup>2p<sub>1/2</sub>). The percentage contribution of Ti2p (Ti<sup>4+</sup> and Ti<sup>3+</sup>) components of the untreated and plasma treated TiO<sub>2</sub>/PET films for different exposure times at 30 W power level, as calculated from Ti2p core level spectra, is shown in Fig. 4c. It can be seen that the surface of the untreated TiO<sub>2</sub>/PET films exhibited a higher concentration of Ti<sup>4+</sup> (Ti<sup>4+</sup>2p<sub>3/2</sub> and Ti<sup>4+</sup>2p<sub>1/2</sub>). After plasma treatment at 30 W, the concentration of Ti<sup>4+</sup> decreased with increasing exposure time, while the concentration of Ti<sup>3+</sup> (Ti<sup>3+</sup>2p<sub>3/2</sub> and Ti<sup>3+</sup>2p<sub>1/2</sub>) on the surface of the TiO<sub>2</sub>/PET films (Fig. 4c) increased. The higher concentration of Ti<sup>3+</sup> in TiO<sub>2</sub>/PET film was achieved when the samples were exposed under higher discharge power of 45 W (Fig. 4d). The above changes may be attributed to desorption of water molecules from the surface of TiO<sub>2</sub>/PET films by ions, electrons, and neutral species and UV radiation in the plasma which can be described as one electron from OH<sup>-</sup> can transfer to the Ti<sup>4+</sup> state and H<sup>+</sup> can take one electron from O<sup>2-</sup> in TiO<sub>2</sub>. Hence, the plasma treated surface mainly exhibited Ti<sup>3+</sup>, O<sup>-</sup> and highly reactive radicals such as H and OH as shown in Scheme 1. The increase in Ti<sup>3+</sup>, O<sup>-</sup> and highly reactive radicals facilitated the improvement in biocompatibility and antibacterial properties of TiO<sub>2</sub>/PET films [25,27,31].

In order to investigate the different oxygen states on the surface of TiO<sub>2</sub>/PET induced by oxygen plasma treatment, a high resolution XPS analysis of O1s peaks was performed. Fig. 5a–b shows the O1s spectra of the untreated sample; deconvoluted in to four peaks at 526.9, 527.9, 529.3 and 525 eV which correspond to the lattice O = in [TiO<sub>2</sub>], -O- in [Ti<sub>2</sub>O<sub>3</sub>], and H<sub>2</sub>O/O(C/H)Ti in [TiO(C/H)Ti] and O<sup>2-</sup> ions in (-Ti-O-



Scheme 1. Mechanism of plasma treatment on the surface of TiO<sub>2</sub>/PET films.

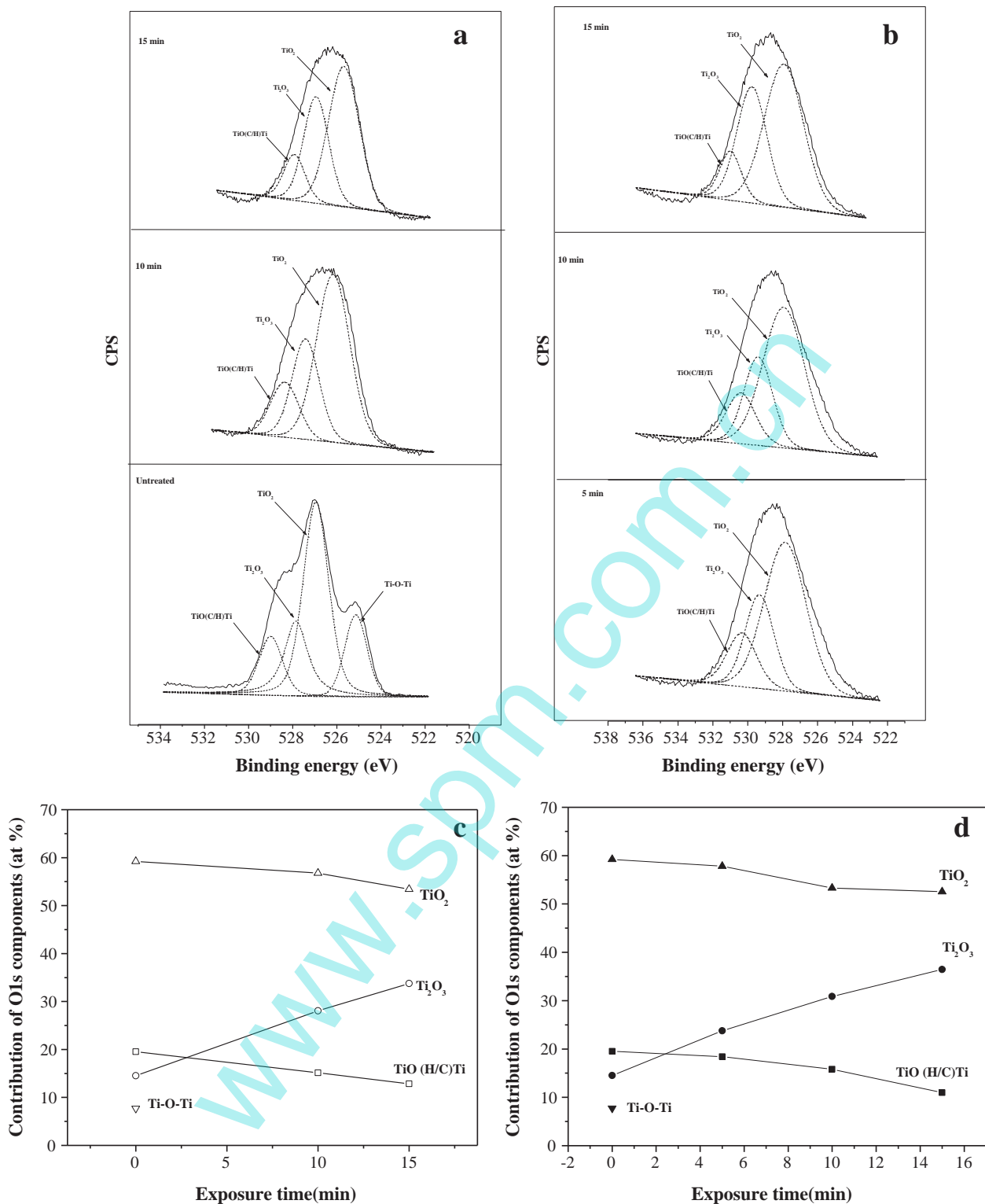


Fig. 5. XPS O1s spectra and contribution of O1s components of O<sub>2</sub> plasma treated TiO<sub>2</sub>/PET film surfaces for different power levels of 30 W (a & c) and 45 W (b & d).

Ti) respectively; the spectra of plasma treated films also showed peaks for TiO<sub>2</sub>, Ti<sub>2</sub>O<sub>3</sub>, TiO (C/H) Ti [29–31]. However, the fourth peak due to –Ti–O–Ti almost disappeared when the sample was treated with oxygen plasma. The concentration of each chemical component with O1s can be calculated by deconvolution using Gaussian–Lorentzian fit; the results are shown in Fig. 5c–d. It is clearly seen that the concentration of the component TiO<sub>2</sub> (Ti<sup>4+</sup> state) and TiO (C/H) Ti

decreased with increasing exposure time at a given power level, whereas Ti<sub>2</sub>O<sub>3</sub> (Ti<sup>3+</sup> state) was found to be increased (Fig. 5c). The higher concentration of Ti<sub>2</sub>O<sub>3</sub> is obtained at a power of 45 W as compared to the power level of 30 W (Fig. 5d). Hence, it was expected that the higher power level of the plasma treatment has increased the TiO<sub>2</sub> active states at the surface. The process of conversion from Ti<sup>4+</sup> state to Ti<sup>3+</sup> is induced by the plasma treatment that can generate oxygen moieties at



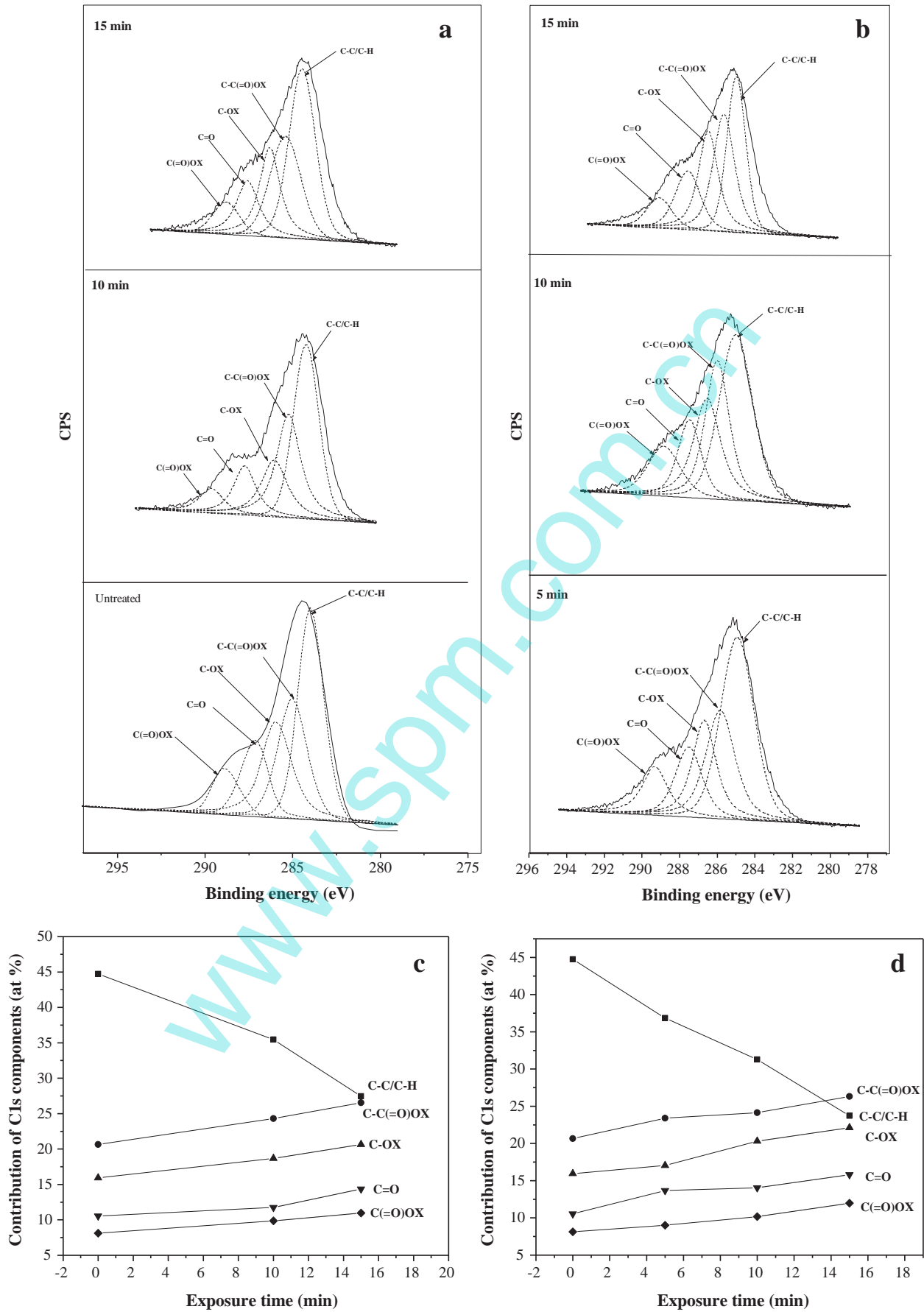


Fig. 6. XPS C1s spectra and contribution of C1s components of O<sub>2</sub> plasma treated TiO<sub>2</sub>/PET film surfaces for different power levels of 30 W (a & c) and 45 W (b & d).

the surface and excess electrons in Ti, this causes the change in the electronic structure of  $\text{TiO}_2$ .

The C1s high resolution XPS spectra of untreated and plasma treated  $\text{TiO}_2/\text{PET}$  films for different treatment times at 30 W are shown in Fig. 6. The spectra of the untreated  $\text{TiO}_2/\text{PET}$  film indicated the presence of five peaks with binding energy of 283.31 for C–C/C–H, 285.3 for C–C(=O)OX, 286.2 for C–OX, 287.6 for C = O and 288.1 eV for C(=O)OX [34] (Fig. 6a). The high resolution spectra of the plasma treated films also showed the peaks at 283.31, 285.3, 286.2, 287.6 and 288.1 eV due to C–C/C–H, C–C(=O)OX, C–OX, C = O and C(=O)OX respectively. It revealed that the intensity of the C–C/C–H component of the plasma treated films decreased while the intensity of oxygen containing functional groups such as C–C(=O)OX, C–OX, C = O and C(=O)OX increased with increasing plasma treatment time. Fig. 6c and d shows the percentage contribution of the C1s components of the plasma treated film. It can be seen that, after the plasma treatment, the C–C groups were found to be decreased, while C–C(=O)OX, C–OX, C = O and C(=O)OX were found to be increased with plasma exposure time. This effect was pronounced for the samples exposed under higher

discharge power of 45 W. These increased oxygen containing functional groups are useful to enhance the biocompatibility and antibacterial properties of the material.

#### 3.4. Bacterial adhesion and cell compatibility analysis

Fig. 7 shows the antibacterial activity of the  $\text{TiO}_2/\text{PET}$  films as a function of exposure time at discharge power level of 45 W which were analyzed against *staphylococcus* bacteria by the inhibition zone method. It was observed that higher concentration of *staphylococcus* bacteria adhered and proliferated on the surface of virgin PET film as shown in Fig. 7a. Comparatively less adhesion and proliferation of bacteria were found on the  $\text{TiO}_2$  immobilized PET film surface as shown in Fig. 7b. Nonetheless, *staphylococcus* bacteria exhibit significantly lower adherence and proliferation on the surface of the oxygen plasma treated  $\text{TiO}_2/\text{PET}$  films (Fig. 7c–e) in comparison to the untreated  $\text{TiO}_2/\text{PET}$  and PET and thus the 15 min treated  $\text{TiO}_2/\text{PET}$  film surface suppressed growth and adhesion of *staphylococcus* bacteria dramatically. The inhibition of bacteria is mainly attributed to the change in chemical state

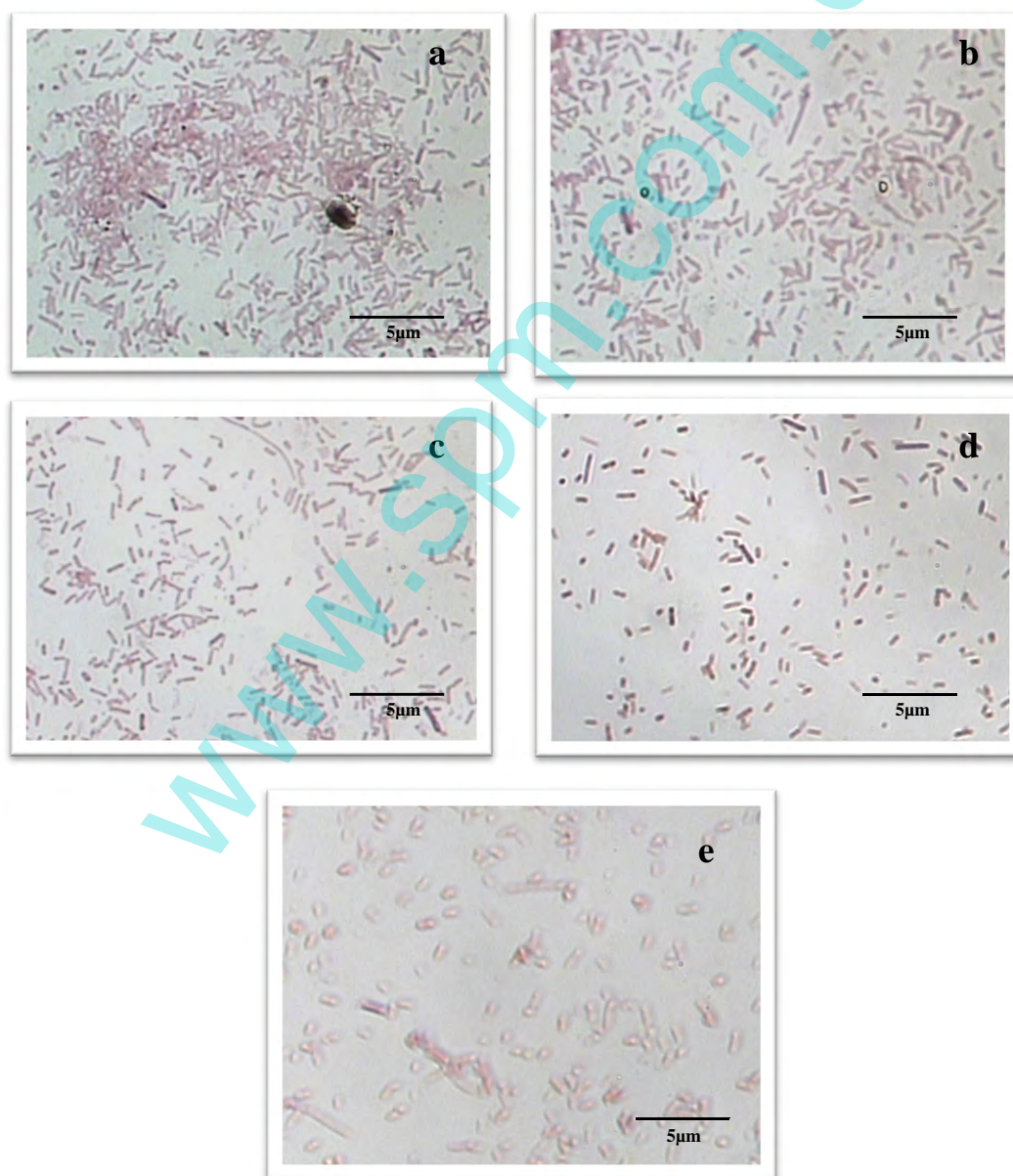


Fig. 7. Optical photograph showing adhesion and proliferation of *staphylococcus* on plasma treated  $\text{TiO}_2/\text{PET}$  film (a) control PET (b) untreated  $\text{TiO}_2/\text{PET}$ , (c) 5 min (d) 10 min and (e) 15 min at the power level of 45 W.

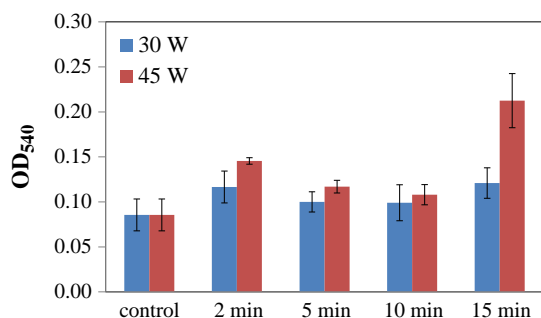


Fig. 8. Osteoblast cell adhesion on plasma treated TiO<sub>2</sub>/PET films as a function of exposure time.

(Ti<sup>4+</sup> → Ti<sup>3+</sup>), incorporation of highly reactive species such as OH<sup>•</sup>, H<sup>•</sup>, O<sup>-</sup> and hydrophilic polar functional groups onto the surface of TiO<sub>2</sub>/PET films by oxygen plasma treatment. The above results clearly demonstrated that the oxygen plasma treated TiO<sub>2</sub>/PET films resist the growth and adhesion of *staphylococcus* bacteria.

The cell compatibility is one of the most significant factors to an initial screening on material toxicity effects against human cells. Cell viability of the plasma treated and untreated TiO<sub>2</sub>/PET films was analyzed by using human osteoblast cells. As indicated in Fig. 8, the OD<sub>540</sub> (absorbance) value of the control TiO<sub>2</sub>/PET film is around 0.08 and it increased considerably at the short exposure (2 min) of oxygen plasma. Interestingly, the values do not change significantly with longer exposure times for the power level of 30 W. However, maximum OD<sub>540</sub> value was observed for the TiO<sub>2</sub>/PET film samples treated at the higher exposure time and discharge power of 45 W, indicating that the plasma treated TiO<sub>2</sub>/PET film (at higher power) possessed good biocompatibility compared with that of the untreated one (control). The absorbance values (OD<sub>540</sub>) are proportional to proliferation cells (cell density) on the surfaces. Therefore, the osteoblast cells showed a higher proliferation rate and cell density on plasma treated TiO<sub>2</sub>/PET films as compared to the untreated one. In other words, cell viability on oxygen plasma treated TiO<sub>2</sub>/PET was superior to that on untreated TiO<sub>2</sub>/PET films due to the formation of high density functional groups and Ti<sup>3+</sup> chemical states as well as surface roughness induced by oxygen plasma treatment [34–36].

#### 4. Conclusion

The transparent TiO<sub>2</sub>/PET films were prepared effectively by simple sol-gel technique. Oxygen glow discharge RF plasma has been used to improve the surface properties of the obtained TiO<sub>2</sub>/PET films. The oxygen plasma treatment incorporated oxygen containing polar functional groups onto the surface of the TiO<sub>2</sub>/PET films caused a decrease in contact angle and increase in surface energy. The increase in surface energy is mainly due to the incorporation of oxygen containing polar components onto the plasma treated TiO<sub>2</sub>/PET film surfaces. The results from the AFM showed a gradual increase in the surface roughness of plasma treated surfaces with exposure time. The XPS results clearly exhibited a decrease in carbon content on the plasma treated film surfaces and significant increase in oxygen and Ti2p on the surface of the TiO<sub>2</sub>/PET films. Furthermore the XPS analysis identified oxygen containing polar groups on the TiO<sub>2</sub>/PET film surfaces and also the increase in the proportion of Ti<sup>3+</sup> in Ti2p whereas a decrease in Ti<sup>4+</sup> state. The increase in surface roughness and concentration of polar functional groups and Ti<sup>3+</sup> states induced by plasma treatment was observed more for the samples treated at higher power level (45 W) and exposure time (15 min). These chemical and morphological changes contributed to enhanced/improved biocompatibility and anti-adhesion bacterial properties of TiO<sub>2</sub>/PET films. This plasma based surface engineering technology has great potential for wide applications in biomedical industry.

#### Acknowledgment

One of the authors (K.N.) would like to express his sincere gratitude to the Science & Engineering Research Board (SERB), Department of Science and Technology (DST), Government of India for providing the financial support and also expresses his deep sense of gratitude to Dr. S. Thangavelu, Chairman, Sri Shakthi Institute of Engineering and Technology for providing available facility to carry out the work in the Department and for his kind encouragement during this work. The authors acknowledge Dr. R. Udhya Kumar, Department of Zoology, Bharathiar University for assisting bacterial adhesion tests and Dr. J. Chandrasekar, Associate Professor, Sri Ramakrishna Mission Vidyala College of Arts and Science for taking thickness measurement of the samples.

#### Notice

The U.S. Environmental Protection Agency, through its Office of Research and Development, funded and managed, or partially funded and collaborated in, the research described herein. It has been subjected to the Agency's administrative review and has been approved for external publication. Any opinions expressed in this paper are those of the author(s) and do not necessarily reflect the views of the Agency, therefore, no official endorsement should be inferred. Any mention of trade names or commercial products does not constitute endorsement or recommendation for use.

#### References

- [1] R. Langer, N.A. Peppas, *AIChE J* 49 (2003) 2990.
- [2] A.E. Madkour, G.N. Tew, *Polym. Int.* 1 (2008) 6.
- [3] W. Zhang, P.K. Chu, J.H. Ji, Y.H. Zhang, X.Y. Liu, R.K.Y. Fu, P.C.T. Ha, Q. Yan, *Biomaterials* 27 (2006) 44.
- [4] W.-S. Wang, X. Wang, X. Fu, J. Weng, Wenyue, *Surg. Coat. Technol.* 205 (2010) 465.
- [5] D. Sakthi Kumar, M. Fujioka, K. Asano, A. Shoji, A. Jayakrishnan, Y. Yoshida, *J. Mater. Sci. Mater. Med.* 18 (2007) 1831.
- [6] T. Matsunaga, Y. Ikada, "Modification of Polymers", in: C.E. Carraher, M. Tsuda, C.E. Carraher, M. Tsuda (Eds.), *ACS Symposium Series*, 121, 1980, p. 391.
- [7] C. Yao, X.S. Li, K.G. Neoh, Z.L. Shi, E.T. Kang, *J. Membr. Sci.* 320 (2008) 259.
- [8] Alenka Vesel, Miran Mozetic, *Vacuum* 86 (2012) 634.
- [9] J. Behnisch, A. Hollander, H. Zimmermann, *J. Appl. Polym. Sci.* 49 (1993) 117.
- [10] S. Bhowmik, P.K. Ghosh, S. Ray, S.K. Barthwal, *J. Adhes. Sci. Technol.* 12 (1998) 1181.
- [11] M.R. Yang, K.S. Chen, J.C. Tsai, C.C. Tseng, S.F. Lin, *Mater. Sci. Eng. C* 20 (2002) 167.
- [12] P. Favia, R. D'Agostino, *Surf. Coat. Technol.* 98 (1998) 1102.
- [13] D.J. Balazs, K. Triandafillou, P. Wood, Y. Chevolut, C.V. Delden, H. Harms, C. Hollenstein, H.J. Mathieu, *Biomaterials* 25 (2004) 2139.
- [14] S. Bhowmik, T.K. Chaki, S. Ray, F. Hoffman, L. Dorn, *Metall. Mater. Trans. A* 35 (2004) 865.
- [15] K.N. Pandiyaraj, V. Selvarajan, R.R. Deshmukh, C. Gao, *Appl. Surf. Sci.* 255 (2009) 3965.
- [16] R.R. Deshmukh, N.V. Bhat, *Mater. Res. Innov.* 7 (2003) 283.
- [17] R. Pareek, A.S. Joshi, P.D. Gupta, P.K. Biswas, S. Das, *Opt. Laser Technol.* 37 (2005) 369.
- [18] J. Szczyrbowski, G. Brauer, G. Teschner, A. Zmely, *Surf. Coat. Technol.* 98 (1998) 1460.
- [19] A. Fujishima, T.N. Rao, D.A. Tryck, *J. Photochem. Photobiol. C Photochem. Rev.* 1 (2000) 1.
- [20] F.M. Fowkes, *J. Phys. Chem.* 67 (1963) 2538.
- [21] R.R. Deshmukh, A.R. Shetty, *J. Appl. Polym. Sci.* 107 (2008) 3707.
- [22] K. Navaneetha Pandiyaraj, J. Heeg, C. Mewes, M. Wienecke, T. Barfels, V. Uthayakumar, *Pi Guey Su, Key Eng. Mater.* 52 (2012) 191.
- [23] K. Navaneetha Pandiyaraj, V. Selvarajan, R.R. Deshmukh Changyou Gao, *Vacuum* 83 (2009) 332.
- [24] N.V. Bhat, D.J. Upadhyay, R.R. Deshmukh, S.K. Gupta, *J. Phys. Chem.* 107 (2003) 4550.
- [25] E. Selli, G. Mazzone, C. Oliva, F. Martin, C. Riccardi, R. Barni, B. Marcandalli, M.R. Massafra, *J. Mater. Chem.* 11 (2001) 1985.
- [26] T. Oktom, N. Seventekin, H. Ayhan, E. Piskin, *Indian J. Fibre Text. Res.* 27 (2002) 161.
- [27] B. Gupta, J. Hilborn, Ch. Hollenstein, C.J.G. Plummer, R. Houriet, N. Xanthopoulos, *J. Appl. Polym. Sci.* 78 (2000) 1083.
- [28] R.N. Wenzel, *Ind. Eng. Chem.* 28 (1936) 988.
- [29] In: K.L. Mittal (Ed.), *Contact Angle, Wettability and Adhesion*, VSP, The Netherlands, 2003.
- [30] M. Modic, I. Junkar, Alenka Vesel, Miran Mozetic, *Surf. Coat. Technol.* 213 (2012) 98.
- [31] J. Jun, M. Dhayal, Joong-Hyeok Shin, Jo-Chun Kim, Nikola Getoff, *Radiat. Phys. Chem.* 75 (2006) 583.
- [32] J. Jun, J.-H. Shin, Marshal Dhayal, *Appl. Surf. Sci.* 252 (2006) 3871.
- [33] P. Zhang, B.K. Tay, Y.B. Zhang, S.P. Lau, K.P. Yung, *Surf. Coat. Technol.* 198 (2005) 184.
- [34] G. Beamson, D. Briggs, *High Resolution XPS of Organic Polymers*, The ScientaESCA300 Database, Wiley, Chichester, 1992.
- [35] C. Ohtsuki, H. Iida, S. Nakamura, A. Osaka, *J. Biomed. Mater. Res.* 35 (1997) 39.
- [36] C. Brunot, L. Ponsonnet, Christelle Lagneau, Pierre Farge, Catherine Picart, Brigitte Grosgeat, *Biomaterials* 28 (2007) 632.